

Controlling the magnetization reversal in planar nanostructures with wire-ring morphology

R. M. Corona, A. Aranda, J. L. Palma, C. E. Lopez, and J. Escrig

Citation: [Applied Physics Letters](#) **105**, 082406 (2014); doi: 10.1063/1.4894292

View online: <http://dx.doi.org/10.1063/1.4894292>

View Table of Contents: <http://scitation.aip.org/content/aip/journal/apl/105/8?ver=pdfcov>

Published by the [AIP Publishing](#)

Articles you may be interested in

[Magnetization reversal behavior in complex shaped Co nanowires: A nanomagnet morphology optimization](#)
J. Appl. Phys. **116**, 193904 (2014); 10.1063/1.4901999

[Kondorski reversal in magnetic nanowires](#)
J. Appl. Phys. **115**, 17D137 (2014); 10.1063/1.4865975

[Tuning the magnetization reversal process of FeCoCu nanowire arrays by thermal annealing](#)
J. Appl. Phys. **114**, 043908 (2013); 10.1063/1.4816479

[Directional-dependent coercivities and magnetization reversal mechanisms in fourfold ferromagnetic systems of varying sizes](#)
J. Appl. Phys. **113**, 013901 (2013); 10.1063/1.4772459

[Magnetization reversal in nanowires with a spiral shape](#)
J. Appl. Phys. **104**, 013906 (2008); 10.1063/1.2948939



Controlling the magnetization reversal in planar nanostructures with wire-ring morphology

R. M. Corona,¹ A. Aranda,¹ J. L. Palma,¹ C. E. Lopez,^{1,2} and J. Escrig^{1,2}

¹Departamento de Física, Universidad de Santiago de Chile (USACH), Av. Ecuador 3493, Santiago, Chile

²Center for the Development of Nanoscience and Nanotechnology (CEDENNA), Av. Ecuador 3493, Santiago, Chile

(Received 22 July 2014; accepted 19 August 2014; published online 27 August 2014)

Magnetization reversal in planar nanowires has been controlled using structures with a larger area pad connected to a nanowire or by means of patterned variations in the planar nanowire such as notches. In this letter, we have introduced a magnetic nanostructure defined as a planar nanostructure with wire-ring morphology. In particular, we have performed micromagnetic simulations to investigate how the magnetic properties (coercivity and remanence) change as a function of the geometric parameters of the nanostructure. Additionally, we observe that when the ring is very thin, the system reverses its magnetization by nucleation and propagation of domain walls along the nanowire. Conversely, when the ring has very thick walls, or directly turns into a solid cylinder, the system nucleates a vortex in the ring/cylinder, and then propagates the domain walls toward the nanowire sections. This reversal process is characterized by a step or plateau in the hysteresis curve, that is, a region in which differential magnetic susceptibility presents a local minimum or, ideally, vanishes. Finally, this nanostructure can be used in many potential applications related to the control of domain walls in planar nanowires. © 2014 AIP Publishing LLC.

[<http://dx.doi.org/10.1063/1.4894292>]

Ferromagnetic planar nanowires patterned lithographically have received increasing interest in recent years because they can effectively act as conduits for propagation of domain walls.¹ Thus, they are the basis for many proposed applications including both magnetic logic^{2,3} and sensor⁴ devices and more recently in magnetic memory concepts.^{5–7} Domain walls have been considered as quasiparticles⁸ that can be controlled by external magnetic fields and spin-polarized currents.

On one hand, domain wall propagation can be controlled using structures with a larger area pad of magnetic material connected to a narrower nanowire of interest.⁹ Such structures have been widely used for injecting domain walls into nanostructures.^{9–13} In particular, O'Shea *et al.*¹⁴ investigated a diamond shaped nucleation pad attached to a nanowire containing a triangular shaped pinning site. They demonstrated that the major advantage of using this type of structure is that the position of the nucleated domain wall is highly reproducible. Besides, Allwood *et al.*¹⁵ investigated a device geometry that acts as a domain wall diode (an isosceles, right-angle triangle with a 500 nm base length, fabricated with its apex joining a 200-nm-wide wire and its base connected to a 100-nm-wide wire).

On the other hand, lithographically patterned variations in the planar nanowire, such as notches, can produce a pinning potential-energy landscape^{10,16–18} creating multiple domains, and hence multiple memory states which could be read out either sequentially in shift registers^{2,19} or directly if an entire nanowire forms the free layer of a magnetic random access memory (MRAM) cell.²⁰ Thus, detailed knowledge of the magnetic properties of planar nanowires with larger area pad or different notches is a vital step toward understanding the fundamental properties of domain walls, and

also toward the optimization of domain wall pinning behavior that is required for magnetic memory devices. Another alternative to control the domain wall propagation is to induce pinning potentials created by inter-domain wall magnetostatic interactions in planar magnetic nanowires,²¹ but for now we will focus our efforts in isolated systems.

The magnetic configuration of a nanostructure is the result of a process of energy minimization that considers both the nanowire geometry as well as the material of which it is composed. In polycrystalline Permalloy (nominal Ni₈₀Fe₂₀) nanowires, the weak magnetocrystalline anisotropy and small magnetostriction allow the magnetization to be largely constrained by magnetostatic energy considerations so as to lie along the long axis of the wire with spins parallel to the surfaces and edges. The magnetization direction in such magnetically soft nanowires is defined by the geometry of the nanowire, and when a nanoring is patterned within the nanowire, the spin structure tends to follow the local edges of this nanoring.²² As magnetostatic energy is dominant for materials with weak magnetocrystalline anisotropy and negligible magnetostriction, it is reasonable to suppose that varying the ring geometry will allow for modification of the magnetic properties of the planar nanowire, so we would expect different mechanisms of magnetization reversal depending on the geometrical structure of the nanoring. Thus, planar nanostructures with wire-ring morphology have additional degrees of freedom (diameter and wall thickness of the ring) to control the pinning and may be exploited in future magnetic memory.

Following these ideas, in this letter, we have introduced this planar nanostructure with wire-ring morphology, as shown in Figure 1. In particular, we have performed micromagnetic simulations to investigate the magnetic reversal

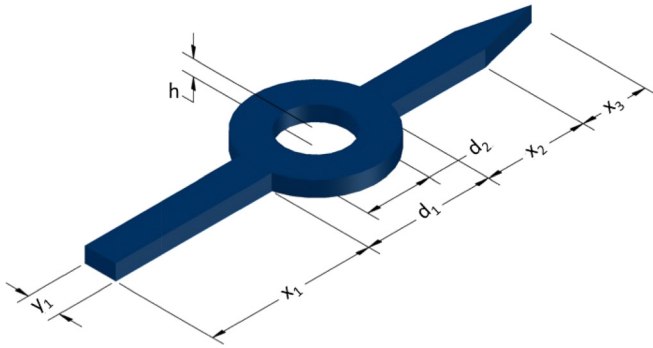


FIG. 1. Geometric characterization of a planar nanostructure with wire-ring morphology.

process in these nanostructures. We focus on the behavior of the coercivity H_c and remanence M_r , concluding that changing the geometry of these nanoparticles enables us to control their magnetic properties. This geometry could be extremely useful in the design of future experiments and devices.

We investigate the hysteresis loops for non-interacting planar nanostructures with a wire-ring morphology using a micromagnetic simulator.²³ This planar nanostructure has a thickness h , which varies between 25 and 100 nm and is composed of three structures: the first is a planar nanowire with length $x_1 = 250$ nm and width $y_1 = 50$ nm. The second structure is a nanoring that has an outer diameter $d_1 = 100$ nm and an inner diameter d_2 variable. The third structure is another planar nanowire with lengths $x_2 = 150$ nm and $x_3 = 100$ nm. The tip shape with length x_3 has been introduced to make harder the nucleation of a domain wall at this end of the nanowire. In this way, we ensure that the magnetization reversal is initiated either from the other end of the nanowire or from the central nanoring, as a function of the geometric parameters of the system. The ratio $\beta = d_2/d_1$ is defined such that $\beta = 0$ represents a solid dot and $\beta \rightarrow 1$ corresponds a very narrow ring. In our particular case, we have varied β between 0.0 and 0.9.

All of the simulations utilized a 2 nm mesh, small enough to be less than the exchange length (in the case of Permalloy it is 5.29 nm), and employed standard magnetic parameters for Permalloy including saturation magnetization $M_s = 860 \times 10^3$ A/m, exchange energy constant $A = 13 \times 10^{-12}$ J/m, and zero magnetocrystalline anisotropy, which is a reasonable representation of polycrystalline $\text{Ni}_{80}\text{Fe}_{20}$.²⁴ The simulations were performed in a quasi-static regime with the damping parameter α in the Landau-Lifshitz-Gilbert equation²⁵ set to 0.5 to speed up the simulations. Besides, in all simulations, we have considered an external magnetic field applied along the major axis of the nanowire.

Figure 2 shows the hysteresis curves of planar nanostructures with wire-ring morphology for $h = 25$ nm (a), $h = 50$ nm (b), and $h = 100$ nm (c) as a function of the wall thickness of the ring, characterized by the parameter β . From this figure, we observe that the hysteresis curves are quite square, exhibiting a remanence close to one and an abrupt change of the magnetization, which realizes the axis of easy magnetization along which is being applied the external magnetic field. Moreover, we can clearly notice that as we increase the thickness h of the nanostructure (from 25 to

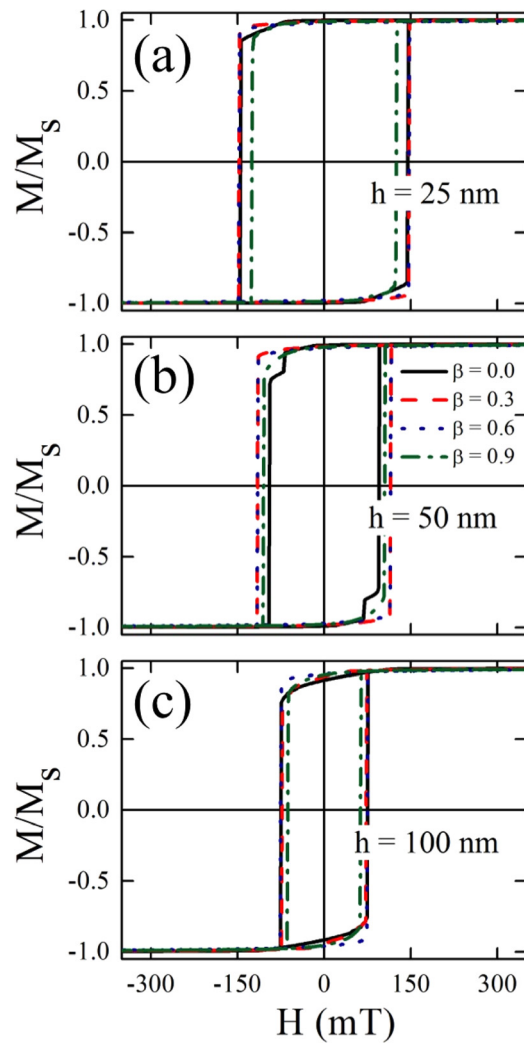


FIG. 2. Hysteresis curves of planar nanostructures with wire-ring morphology for $h = 25$ nm (a), $h = 50$ nm (b), and $h = 100$ nm (c) as a function of β .

100 nm), the coercivity decreases regardless of the β value. The most interesting effect from these hysteresis curves occurs for $h = 50$ nm and $\beta = 0.0$ (a solid cylinder). This curve clearly shows two well-defined Barkhausen jumps defining a small plateau that owes its origin to the ring reversing its magnetization first, then the nanowire (see Figure 4(a)). Similar hysteresis curves are obtained for $\beta \leq 0.2$. On the contrary, for $\beta \geq 0.3$, the two Barkhausen jumps become one, eliminating the plateau, which indicates that the nanostructure reverses its magnetization from one of its end (see Figure 4(b)).

In Figure 3, we summarize the coercivity H_c and normalized remanence M_r/M_s obtained from our simulations for different β values. From Figure 3(a), we can verify that the coercivity decreases as we increase the thickness h of the nanostructure. Moreover, we observed that the coercivity is almost constant regardless of the β value. The only significant break occurs for β values between 0.2 and 0.3. Clearly, at this point there is a change in the mechanism of magnetization reversal of the system (see Figure 4), a fact that had been reflected above as the appearance and disappearance of a plateau in the hysteresis curve of the nanostructure for $h = 50$ nm (see Figure 2(b)). Importantly, this nanostructure is presented as promising for potential applications, since

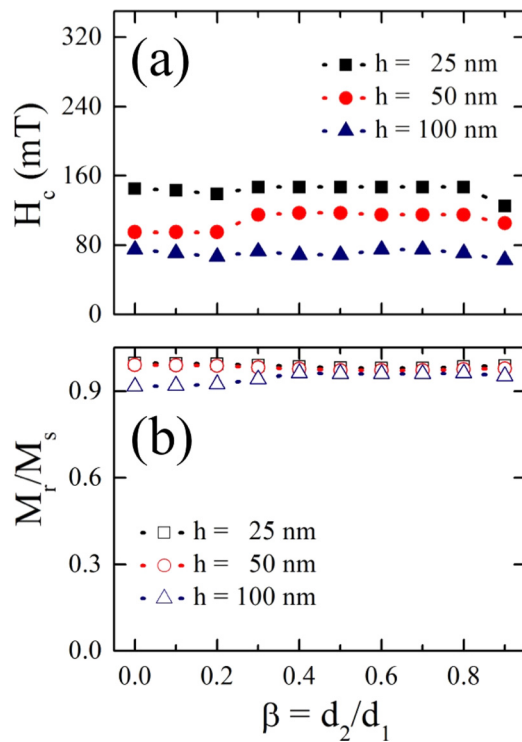


FIG. 3. Coercivity (a) and normalized remanence (b) for planar nanostructures with wire-ring morphology as a function of β .

varying the wall width of the ring we can control the mechanism of magnetization reversal keeping approximately constant the coercivity.

Figure 3(b) shows the normalized remanence as a function of β for different thicknesses h of the nanostructure. From this figure, we observe clearly higher remanence values (between 0.9 and 1.0) independently of β and the thickness of the nanostructure. This is a clear indication that the system remains a nanowire with a strong shape anisotropy along the same, regardless of the existence of a ring. Besides, the lowest values of remanence occur for $h = 100$ nm and $\beta < 0.3$. A decrease in remanence as a function of thickness of the nanowires had been previously observed by Goolaup *et al.*²⁶ However, in this case, we observed that the remanence changes as a function of β , which is a clear indication that the system reverses its magnetization differently as a function of

the hole of the ring, in accordance with measurements previously obtained for the coercivity.

Finally, to better understand the appearance of a plateau in the hysteresis curve (see Figure 2(b)) and the abrupt transition in the coercivity for β values between 0.2 and 0.3 (see Figure 3(a)), we show snapshots of the magnetization reversal for planar nanostructures with wire-ring morphology. In particular, we consider nanostructures with $h = 50$ nm and β varying between 0.2 and 0.3. As we discussed previously for β values lower than 0.3, the hysteresis curves show a plateau. Figure 4(a) shows the magnetic configuration obtained in the plateau, showing clearly that the magnetization reversal begins by forming a vortex in the ring which is fairly stable (indicating the size of the plateau), after which begins to reverse the nanowire. Furthermore, Figure 4(b) shows that for nanostructures with $\beta \geq 0.3$, the system reverses its magnetization by the nucleation of a domain wall in one end of the planar nanowire and the propagation of it through the nanostructure. This magnetization reversal is much steeper than the previous one, thus explaining the disappearance of the plateau in the hysteresis curve, which now has a single Barkhausen jump.

Finally, considering that we have performed micromagnetic simulations in a single magnetically soft material, we would like to emphasize that the appearance of the plateau depends mainly on the geometric parameters of the nanostructure. However, the width of the plateau can also be controlled by using different magnetic materials for the ring and for the nanowire, research we are currently developing.

In conclusion, we have introduced a geometry defined as a planar nanostructure with wire-ring morphology, which enables us to handle the mechanisms of magnetization reversal in planar nanowires. Using micromagnetic simulations, we have investigated the hysteresis curves of these nanostructures as a function of their geometric parameters. Interestingly, we observe the appearance and disappearance of a plateau in the hysteresis curves that produces a change in the value of the coercivity. This behavior is related to a change in the mechanism of magnetization reversal of the nanostructure, associated with a variation in the wall thickness of the ring. For $\beta \leq 0.2$, the system reverses its magnetization by nucleating a vortex in the ring and then reversing the wire magnetization by propagating domain walls. Conversely, for $\beta \geq 0.3$, the system reverses its magnetization only by domain wall propagation. Finally, the strong impact of the geometry in the magnetic behavior of these nanostructures can be useful for tailoring specific magnetic properties, as well as for controlling the movement of domain walls in planar nanowires.

The authors acknowledge financial support from Fondecyt Grant Nos. 3130393, 1110784, and 1121034, Grant ICM P10-061-F by Fondo de Innovación para la Competitividad-Minecon and the Financiamiento Basal para Centros Científicos y Tecnológicos de Excelencia, under Project FB0807. CONICYT Ph.D. Program Fellowships is also acknowledged.

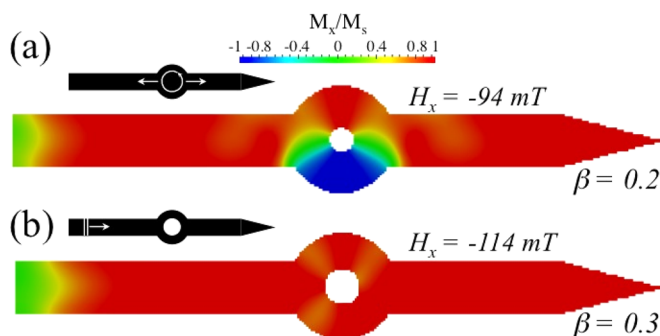


FIG. 4. Snapshots of the stable magnetization state corresponding to a planar nanostructure with wire-ring morphology for $h = 50$ nm and $\beta = 0.2$ (a) and 0.3 (b). The insets are schemes to explain how the process of magnetization reversal occurs in each case.

¹R. P. Cowburn, D. A. Allwood, G. Xiong, and M. D. Cooke, *J. Appl. Phys.* **91**, 6949 (2002).

²D. A. Allwood, G. Xiong, M. D. Cooke, C. C. Faulkner, D. Atkinson, N. Vernier, and R. P. Cowburn, *Science* **296**, 2003 (2002).

- ³D. A. Allwood, G. Xiong, C. C. Faulkner, D. Atkinson, D. Petit, and R. P. Cowburn, *Science* **309**, 1688 (2005).
- ⁴M. Diegel, R. Mattheis, and E. Halder, *IEEE Trans. Magn.* **40**, 2655 (2004).
- ⁵D. A. Allwood, G. Xiong, and R. P. Cowburn, *Appl. Phys. Lett.* **89**, 102504 (2006).
- ⁶D. Atkinson, D. S. Eastwood, and L. K. Bogart, *Appl. Phys. Lett.* **92**, 022510 (2008).
- ⁷S. S. P. Parkin, M. Hayashi, and L. Thomas, *Science* **320**, 190 (2008).
- ⁸M. Klaui, *J. Phys.: Condens. Matter* **20**, 313001 (2008).
- ⁹K. Shigeto, T. Shinjo, and T. Ono, *Appl. Phys. Lett.* **75**, 2815 (1999).
- ¹⁰M. Tsui, R. E. Fontana, and S. S. P. Parkin, *Appl. Phys. Lett.* **83**, 2617 (2003).
- ¹¹D. Atkinson, D. A. Allwood, G. Xiong, M. D. Cooke, C. C. Faulkner, and R. P. Cowburn, *Nat. Mater.* **2**, 85–87 (2003).
- ¹²D. Lacour, J. A. Katine, L. Folks, T. Block, J. R. Childress, M. J. Carey, and B. A. Gurney, *Appl. Phys. Lett.* **84**, 1910 (2004).
- ¹³M. T. Bryan, D. Atkinson, and D. A. Allwood, *Appl. Phys. Lett.* **88**, 032505 (2006).
- ¹⁴K. J. O'Shea, J. Tracey, S. Bramsiepe, and R. L. Stamps, *Appl. Phys. Lett.* **102**, 062409 (2013).
- ¹⁵D. A. Allwood, G. Xiong, and R. P. Cowburn, *Appl. Phys. Lett.* **85**, 2848 (2004).
- ¹⁶L. K. Bogart, D. S. Eastwood, and D. Atkinson, *J. Appl. Phys.* **104**, 033904 (2008).
- ¹⁷L. K. Bogart, D. Atkinson, K. O'Shea, D. McGrouther, and S. McVitie, *Phys. Rev. B* **79**, 054414 (2009).
- ¹⁸D. S. Eastwood, L. K. Bogart, and D. Atkinson, *Acta Physica Polonica A* **118**, 719–722 (2010), available at <http://przyrbwn.icm.edu.pl/APP/PDF/118/a118z5p001.pdf>.
- ¹⁹S. S. P. Parkin, U.S. patent 6,834,005 (21 December 2004).
- ²⁰J. Nickel and M. K. Bhattacharyya, U.S. patent 7,078,244 (18 July 2006).
- ²¹T. J. Hayward, M. T. Bryan, P. W. Fry, P. M. Fundi, M. R. J. Gibbs, M.-Y. Im, P. Fischer, and D. A. Allwood, *Appl. Phys. Lett.* **96**, 052502 (2010).
- ²²P. Landeros, J. Escrig, D. Altbir, M. Bahiana, and J. d'Albuquerque e Castro, *J. Appl. Phys.* **100**, 044311 (2006).
- ²³M. J. Donahue and D. G. Porter, *OOMMF User's Guide, Version 1.0* (Interagency Report NISTIR 6376, National Institute of Standards and Technology, Gaithersburg, MD, 1999).
- ²⁴H. He and N. J. Tao, *Encyclopedia of Nanoscience and Nanotechnology* (American Scientific Publishers, Stephenson Ranch, CA, 2004).
- ²⁵A. Hubert and R. Schafer, *Magnetic domains: The analysis of magnetic microstructures* (Springer, Berlin, 1998).
- ²⁶S. Goolaup, N. Singh, A. O. Adeyeye, V. Ng, and M. B. A. Jalil, *Eur. Phys. J. B* **44**, 259–264 (2005).